ARTICLE

Preparation, Characterization and Photocatalytic Activity of Lanthanum Doped Mesoporous Titanium Dioxide

Zhong-liang Shi[a], Hong Lai[a], Shu-hua Yao[a*], Shao-feng Wang[b*]

a. School of Applied Chemistry, Shenyang University of Chemical Technology, Shenyang 110142, China
b. Institute of Applied Ecology, Chinese Academy of Sciences, Shenyang 110016, China

(Dated: Received on September 2, 2011; Accepted on October 31, 2011)

Lanthanum doped mesoporous titanium dioxide photocatalysts with different La content were synthesized by template method using tetrabutyltitanate ($Ti(OC_4H_9)_4$) as precursor and Pluronic P123 as template. The catalysts were characterized by thermogravimetric differential thermal analysis, N_2 adsorption-desorption measurements, X-ray diffraction, and UV-Vis adsorption spectroscopy. The effect of La^{3+} doping concentration from 0.1% to 1% on the photocatalytic activity of mesoporous TiO_2 was investigated. The characterizations indicated that the photocatalysts possessed a homogeneous pore diameter of about 10 nm with high surface area of 165 m^2/g. X-ray photoelectron spectroscopy measurements indicated the presence of C in the doped samples in addition to La. Compared with pure mesoporous TiO_2, the La-doped samples extended the photoabsorption edge into the visible light region. The results of phenol photodecomposition showed that La-doped mesoporous TiO_2 exhibited higher photocatalytic activities than pure mesoporous TiO_2 under UV and visible light irradiation.

Key words: Mesoporous titanium dioxide, Lanthanum-doping, Photocatalytic activity, Phenol

I. INTRODUCTION

Titanium dioxide (TiO_2) is an effective catalytic material and has been intensively studied for sensors [1, 2], as a photocatalyst [3] in solar cells [4], lithium-ion cells [5], and many others. It is a promising photocatalyst for remediation of organic pollutants in air [6−8] and water [9−12]. Compared with titania, mesoporous TiO_2, which displays better photocatalytic activity because of its high specific surface area and uniform pore diameter, has therefore received much interest in photocatalysis [13, 14]. However, the application of mesoporous TiO_2 is yet limited by the fast recombination of electron-hole pairs and the wide band gap, which corresponds to the UV light [15]. Therefore, the development of visible light responsive mesoporous TiO_2 has the positive effect on improving the photocatalytic efficiency. In addition, for practical application to decompose indoor organic pollutants, it is necessary to extend the photoabsorption of mesoporous TiO_2 into visible light region. Thus, exploring visible light absorption and large surface areas mesoporous TiO_2 is significant.

In order to reduce the electron-hole recombination and sensitization towards visible light, the modification of TiO_2 has been extensively investigated. Metal ion doping has been widely performed on semiconductors to minimize electron/hole recombination and enhance their absorption towards visible light region [16, 17]. However, transition metal doped TiO_2 suffers from a thermal instability or an increase in the carrier recombination centers [18]. Rare earth metals having incompletely occupied 4f and empty 5d orbital often serve as catalyst or promote catalysis. Some results showed that the photocatalytic activity of TiO_2 could be improved by the doping of some rare earth metals [19−21]. Besides, it has been proved that lanthanum, as one of the rare earth metals, has the ability to enhance the photocatalytic activity of TiO_2 [22−25]. Lanthanide doping was proved to increase the surface area, pore volume, adsorption capacity for organic compounds as well as to suppress electron-hole recombination rates during the process of photocatalytic reaction [26, 27]. However, so far, there is no systematic study on the effect of the La/Ti molar ratio on the phenol photodecomposition over La-doped mesoporous TiO_2 under visible light irradiation.

In this work, the synthesis, characterization, and application of La-doped mesoporous TiO_2 (La/MT) particles with series of lanthanum loading were reported. La/MT was synthesized by template method using $Ti(OC_4H_9)_4$ as precursor and Pluronic P123 as template, and extensively characterized using various so-

*Authors to whom correspondence should be addressed. E-mail: ysh1997@163.com

phisticated techniques. The effect of La doping concentration on the photocatalytic activity of mesoporous TiO_2 was investigated from 0.1% to 1% (in mol). The photocatalytic activity was evaluated by photodegradation of phenol over these obtained samples under UV-light and visible light irradiation.

II. EXPERIMENTS

A. Preparation of catalysts

La-doped mesoporous TiO_2 was prepared by template method using Pluronic P123 ($EO_{20}PO_{70}EO_{20}$, Aldrich Chemical Co., Milwaukee, WI) as template and titanium tetraisopropoxide (analytical grade, Shanghai Xingta Co., Ltd., China) and lanthanum nitrate hexahydrate ($La(NO_3)_3{\cdot}6H_2O$) as titanium and lanthanum sources, respectively. In a typical synthesis, 0.01 mol of $Ti(OC_4H_9)_4$ was added to a solution containing 1 g of Pluronic P123 and 10 g of anhydrous ethanol. To this solution, 0.01, 0.05, and 0.10 mmol $La(NO_3)_3{\cdot}6H_2O$ was added for the synthesis of La-doped mesoporous TiO_2, respectively. The resulting sol was gelled in an open petri dish at 50 °C in air for 4 days. The as-made bulk samples were then calcined at 500 °C for 2 h in air at the heating rate of 1 °C/min to remove the surfactant. The calcined samples were labeled according to the La-doping content (denoted as La/MT-0.1, La/MT-0.5, and La/MT-1.0).

B. Characterization

The powder of La/MT-0.5 catalyst was subjected to thermogravimetric differential thermal analysis (DTG-60 TG-DTA, SHIMADZU, Japan) to determine the temperature of possible decomposition and phase change. The crystallinity of all catalysts were analyzed by Rigaku D/max-r B X-ray diffractometer with Cu Kα radiation in the scanning range of 2θ between 20° and 80°. The accelerating voltage and applied current were 40 kV and 40 mA, respectively. Data were recorded at a scan rate of 0.02°/s in the 2θ range of 20°−80°. The size of the crystallite was calculated from X-ray line broadening from the Scherrer equation: $D{=}0.89\lambda/\beta\cos\theta$, where D is the average crystal size in nm, λ is the Cu Kα wavelength (154.06 pm), β is the full-width at half-maximum, and θ is the diffraction angle. Information about specific surface area and pore volume of catalysts was calculated using the BET method [28] from nitrogen adsorption-desorption isotherms measured at 77 K with a Micromeritics 2000 instrument (ASAP 2000, Micromerit-ics, USA). UV-Vis adsorption spectroscopy measurements were performed by a UV-Vis diffuse reflectance spectrophotometer (Shimadzu UV-2550). Reflectance spectra were referenced to $BaSO_4$. A thermo electron corporation theta probe equipped with Mg Kα excitation was employed to measure the presence of elements in La/MT-0.5 photocatalyst. Detailed scans were recorded for Ti2p, O1s, La3d, and C1s.

C. Measurement of photocatalytic efficiency

The photocatalytic activity of the prepared catalysts under UV and visible light was estimated by measuring the degradation rate of phenol (20 mg/L) in an aqueous solution without concerning the degradation intermediates in detail.

The photoreaction was carried out using a magnetically stirred quartz reactor and an ultraviolet mercury lamp (150 W, 365 nm) at ambient temperature of about 20 °C. The pH of the suspension was adjusted either with dilute 0.1 mol/L HCl or 0.1 mol/L NaOH. 60 min adsorption time in dark condition was allowed before the start of photoreactions. Then, samples of the suspension were withdrawn after a definite time interval and filtered through 0.45 μm filter paper. The filtrate was analyzed by a total organic carbon (TOC) analyzer (Shimadzu, 5000A) equipped with a single injection auto sampler (ASI-5000) to find out the extent of mineralization of phenol, and the residual phenol concentration using a UV-Vis spectrophotometer (UV762, Shanghai Analysis Co.) at 269.5 nm. In order to compare the photocatalytic activity of La-doped mesoporus TiO_2, the pure mesoporus TiO_2 powders were also tested. The amount of mesoporus TiO_2 powders was chosen as 1.0 g/L, which was adequate under our conditions without disturbing the UV light entering the reactor.

The experiments with visible light irradiation were performed at ambient temperature of about 20 °C by a 150 W metal halide lamp as the light source. To limit the irradiation wavelength, the light beam was passed through a 410 nm cut filter (L41) to assure cut-off wavelengths shorter than 410 nm. Then, samples of the suspension were withdrawn after a definite time interval and filtered through 0.45 μm filter paper.

III. RESULTS AND DISCUSSION

A. Thermal analysis

Figure 1 shows the DTA and TG thermodiagrams for the La/MT-0.5 sample. It could be seen from Fig.1 that the weight of sample sharply decreased up to 400 °C, and slowly decreased from 400 °C to 700 °C. DTA analysis also showed the endothermic peak at 100 °C and exothermic peak at 500 °C. It was thought that the peak at 100 °C was due to free adsorbed water, and the peak at 500 °C was due to the crystallization of the amorphous phase into the anatase phase. Above 500 °C, it could be assumed that the product completely transforms into the anatase phase because there was no change in particle weight. No significant thermal effects of the transformation of the anatase phase into the rutile phase were detected even up to 700 °C.

DOI:10.1088/1674-0068/25/01/96-102

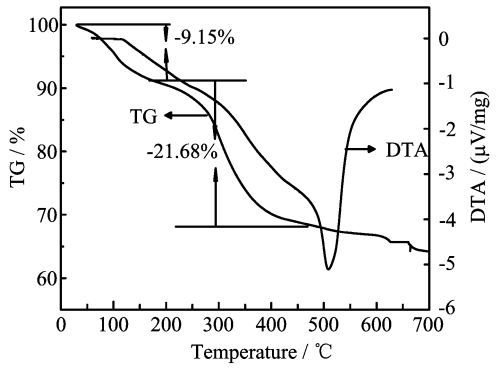

FIG. 1 DTA-TG curve for La/MT-0.5 catalyst.

B. XRD analysis

To obtain information on the crystal structure of the La/MT photocatalysts, X-ray diffraction (XRD) patterns were measured. The XRD patterns of prepared samples were shown in Fig.2, XRD analysis reveal that pure mesoporus TiO_2 and La-doped mesoporus TiO_2 catalysts were composed of both anatase and rutile phases, whereas prepared catalysts also contained brookite as a minor phase. A small peak at 30.8° corresponds to the (121) diffraction peak of brookite phase. The presence of this phase caused the slight shift to a higher angle of the anatase (101) peak since there was overlapping brookite (120) and (111) peaks [29, 30]. The diffraction pattern of La-doped mesoporus TiO_2 photocatalysts was similar to that of pure mesoporus TiO_2. No characteristic peak of La oxide was found in the XRD patterns implying either La ions were incorporated in the crystallinity of TiO_2, or La oxide was very small and highly dispersed.

In addition, the mean crystallite size was calculated as a function of peak width, specified as the full width at half maximum peak intensity based on the Scherrer equation. The physical properties determined from XRD data of the samples were listed in Table I. The crystallite size decreased because of the doping, which implied that La doping restrained the increase in grain size and refines crystallite size. The change of crystal parameters became great in the doping samples compared with un-doping implied crystal matrix that could be expanded. In fact, it seems impossible for La^{3+} to really cooperate with the matrix of TiO_2 because of the mismatch of the ionic radii of Ti^{4+} and La^{3+}. It is expected that the surrounding lanthanum ions will inhibit the phase transition of anatase-rutile through the formation of a Ti−O−La bond. On the other hand, the La_2O_3 lattice locks the Ti−O species at the interface with TiO_2 domains, preventing the nucleation that is necessary for the transformation of anatase to rutile, and results in the decrease of the crystallite size of TiO_2 [31].

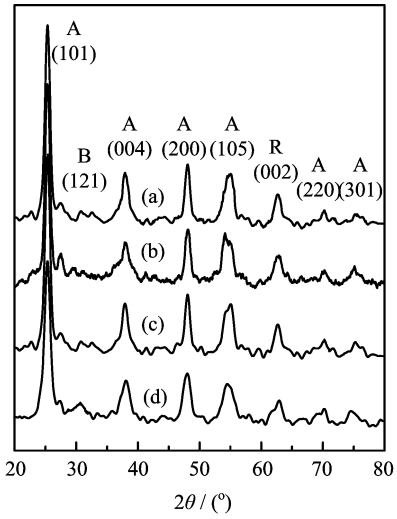

FIG. 2 XRD patterns of samples. The peaks marked "A", "R", and "B" correspond to anatase, rutile, and brookite phase, respectively. (a) La/MT-0.1, (b) La/MT-0.5, (c) La/MT-1.0, and (d) mesoporous TiO_2.

TABLE I XRD analysis results of samples.

Sample	Crystallite size/nm	Lattice parameters		
		a/nm	c/nm	V/nm^3
Mesoporous TiO_2	11.4	0.3776	0.9486	0.1353
La/MT-0.1	10.6	0.3788	0.9493	0.1362
La/MT-0.5	10.3	0.3791	0.9498	0.1365
La/MT-1.0	9.7	0.3785	0.9515	0.1363

TABLE II The physicochemical properties of La-doped mesoporous TiO_2.

Sample	S_{BET}/(m^2/g)	V_t[a]/(m^3/g)	d[b]/nm
Mesoporous TiO_2	154.0	0.326	12.8
La/MT-0.1	155.7	0.337	11.3
La/MT-0.5	165.9	0.383	10.1
La/MT-1.0	156.6	0.339	10.6

[a] Total pore volume.
[b] Average pore diameter.

C. Nitrogen adsorption-desorption analysis

Information about specific surface area, pore volume and BET surface area of catalysts were summarized in Table II. Measured BET surface areas of La-doped samples had higher surface than pure mesoporous TiO_2, the La/MT-0.5 sample displayed the highest specific surface area 165.91 m^2/g and the highest pore volume 0.383 cm^3/g. When the La/Ti percentage increased beyond 0.50%, a decrease in the surface area was observed. The large surface area and pore of La-doped mesoporous TiO_2 can allow an easy diffusion of the pollutant molecules in and around the semiconductor, thus enhancing the adsorption of pollutant molecules

DOI:10.1088/1674-0068/25/01/96-102

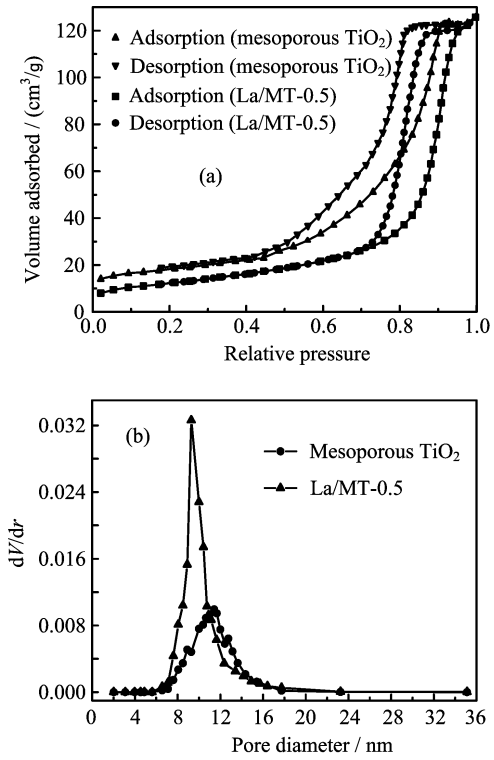

FIG. 3 (a) N_2 adsorption-dcsorption isotherms and (b) BJH pore size distributions of pure mesoporous TiO_2 and La/MT-0.5.

and its intermediate on the surface of the catalysts. The N_2 adsorption-desorption isotherms and Barret-Joyner-Halenda (BJH) pore size distribution plots (calculated from the adsorption branch) of pure mesoporous TiO_2 and La/MT-0.5 catalyst were shown in Fig.3. The adsorption-desorption isotherms of all samples are of type IV with H_2 hysteresis loop with stepwise adsorption and desorption [32]. The sharp decline in the desorption curve and the hysteresis loop at high relative pressure are indicative of mesoporosity. During the process of adsorption, single molecular layer adsorption occurred at relatively low pressure and then multimolecular layer adsorption occurred at higher pressure. The larger the sample pore sizes are, the higher the pressure of capillary cohesion occurs [33]. As shown in Fig.3, the capillary cohesion of mesoporous TiO_2 occurred at the higher pressure and that of La/MT-0.5 occurred at the lower pressure. It suggested that the mesoporous TiO_2 had the larger pore size and La/MT-0.5 had the smaller pore size. The narrow pore size distribution curves indicated that the present materials have uniform pore channels. The narrow pore size distribution was not affected by the La-doping.

D. UV-Vis absorption spectra analysis

UV-Vis absorption spectra were used to characterize the light absorption ability of the prepared photocatalysts. Figure 4 shows the UV-Vis absorption spectra of different samples that show the influence of La ion on the UV-Vis absorption. Modification of mesoporous TiO_2 with La ion significantly affected the absorption property of photocatalysts. It was noticeable that a light absorption in the visible region (420−700 nm) of the modified mesoporous TiO_2 was higher than that of mesoporous TiO_2, and the light absorption increased with increasing La ion content. Modification of La caused the absorption spectra over the sample to shift to the visible region demonstrating that La-doping was in favor of visible-light absorption. For pure TiO_2, the absorption in the ultraviolet range (λ=378 nm) is associated with the excitation of the O2p electron to the Ti3d level. It was thought that the red shift was caused by the new energy level in the band gap. The red shift of the absorption spectrum could be ascribed to the charge transfer between the TiO_2 valence or conduction band and the La ion 4f level [21]. As a result, the La-doped sampless have trapping level which decreased the TiO_2 band gap, and the La ions in the doped photocatalysts increased the visible light absorption ability of the photocatalysts. Moreover, because of rare earth elements possessing a broad absorption band, the effect of those incorporated into the TiO_2 was similar to the influence of adding a photosensitizer to the reaction solution. Therefore, the La ions surrounding the TiO_2 grains could absorb a larger range of light radiation, which brought about the higher light absorption in the 420−700 nm region for the La-doped samples [34]. This extended absorbance indicated the possible enhancement in the photocatalytic activity of mesoporous TiO_2 illuminated by visible light.

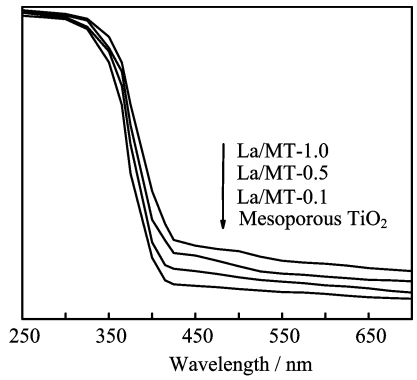

FIG. 4 UV-Vis absorption spectra of samples.

E. X-ray photoelectron spectroscopy analysis

X-ray photoelectron spectroscopy (XPS) spectrum of Ti2p of La/MT-0.5 is shown in Fig.5(a). Ti2p peak appeared as a single, well defined, spin-split doublet with the typical interval of 6 eV between its two peaks which corresponds to Ti^{4+} in a tetragonal structure (*i.e.*, $Ti2p_{1/2}$ and $Ti2p_{3/2}$). The binding energies of

DOI:10.1088/1674-0068/25/01/96-102

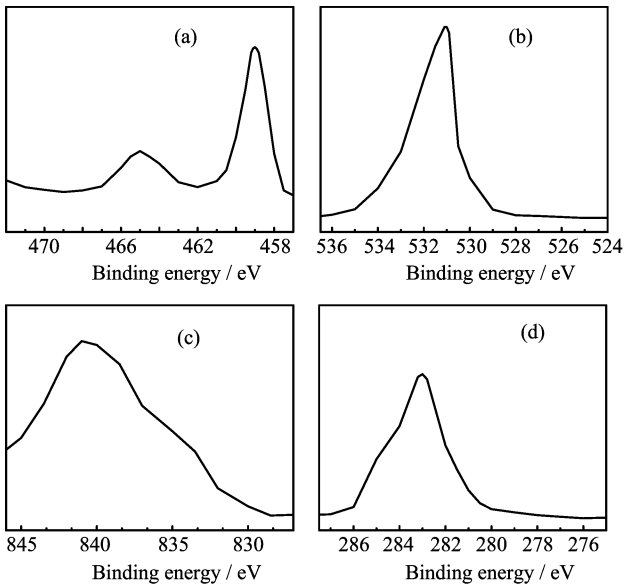

FIG. 5 XPS spectra of La/MT-0.5. (a) Ti2p, (b) O1s, (c) La3d, and (d) C1s.

the peaks within the doublet were found to be 465.1 eV for $Ti2p_{1/2}$ and 459.2 eV for $Ti2p_{3/2}$ signal. The XPS spectrum of O of TiO_2 is shown in Fig.5(b). An intense signal at about 531.2 eV is due to O^{2-} of TiO_2. This peak was attributed to the Ti−O in TiO_2 and OH groups on the surface of the catalysts [35, 36]. The XPS spectrum of La3d is shown in Fig.5(c). La^{3+} that incorporated into TiO_2 lattice makes interaction with oxidic sites of TiO_2 (Ti−O−La) and appears to provide a broadened spectrum of La3d. The XPS spectrum of C1s is shown in Fig.5(d), the C1s spectrum was composed of two peaks (about 283 and 285 eV). The peaks were assigned to the C1s signals due to the Ti−C bond (281.9 eV) and C−C bond (285.3 eV), respectively [37, 38]. So, it can be concluded that the Ti, O, La, and C elements were present in La-doped mesoporous TiO_2. The presence of C elements may be the reason that pure mesoporous TiO_2 showed photocatalytic activity under visible light irradiation [39].

F. Photocatalytic activity

In order to evaluate the actual photocatalytic activity of the La-doped mesoporous TiO_2 photocatalyst calcined at 500 °C for 2 h. Four phenol removal processes, namely, photolysis, photocatalytic degradation by mesoporous TiO_2, La/MT-0.5, and adsorption of La/MT-0.5 were compared and shown in Fig.6. The corresponding experiments to assess the effect of catalyst on the overall removal rate for an initial phenol concentration of 20 mg/L, were also given.

Experimental results shows that phenol could be degraded at a certain degree under UV irradiation (see Fig.6(a)). The La/MT-0.5 sample shows a little adsorption ability to phenol, but the adsorption of phenol on La/MT-0.5 got saturated after 120 min, the removal of phenol did not increase any more with the prolonging of time (Fig.6(b)). The phenol degradation rates increased with UV light irradiation for the phenol/mesoporous TiO_2 system and phenol/La/MT-0.5 system, but the degradation percentages of phenol with La/MT-0.5 are higher than those of mesoporous TiO_2 (Fig.6 (c) and (d)). By comparison of the amounts of phenol removed with and without UV (Fig.6), it can be affirmed that the disappearance of phenol molecules was due to photocatalytic degradation instead of only adsorption.

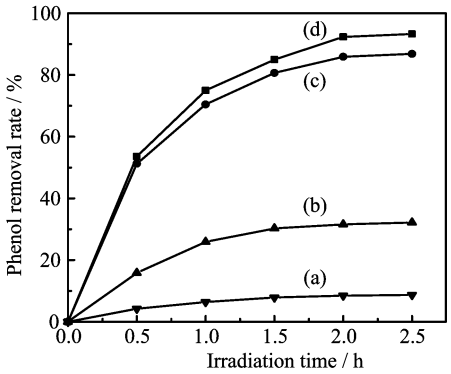

FIG. 6 Effect of photocatalyst on the degradation rate of phenol. (a) Phenol only with UV irradiation, (b) La/MT-0.5 without UV irradiation, (c) mesoporous TiO_2 with UV irradiation, and (d) La/MT-0.5 with UV irradiation.

Photocatalytic activity of La-doped mesoporous TiO_2 powders was estimated by measuring the mineralization extent of phenol in the presence of UV and visible light irradiation without concerning the degradation intermediates in detail. Pure mesoporous TiO_2 synthesized by the same method without any dopant was used as the reference system.

The plot of TOC value of phenol with irradiation time under UV-light irradiation in the presence of La/MT photocatalysts with La-doped content in the range of 0.10%−1.0% is illustrated in Fig.7. It can be clearly seen from the Fig.7 that the decrease of TOC concentration of phenol for La/MT was relatively higher compared to pure mesoporous TiO_2. Decrease of TOC value of phenol showed maximum for La/MT-0.5. It was thought that doped metal ions influence the photocatalytic activity of TiO_2 by acting as electron (or hole) traps and by altering e^-/h^+ pair recombination rate through the following processes:

$$TiO_2 + h\nu \rightarrow TiO_2(h^+_{vb} + e^-_{cb}) \quad (1)$$

$$M^{n+} + h\nu \rightarrow M^{(n-1)+} + h^+_{vb} \quad (2)$$

$$M^{n+} + h\nu \rightarrow M^{(n+1)+} + e^-_{cb} \quad (3)$$

$$h^+_{vb} + M^{n+} \rightarrow M^{(n+1)+} \quad (4)$$

$$e^-_{cb} + M^{n+} \rightarrow M^{(n-1)+} \quad (5)$$

$$h^+_{vb} + e^-_{cb}(TiO_2) \rightarrow TiO_2 \quad (6)$$

DOI:10.1088/1674-0068/25/01/96-102

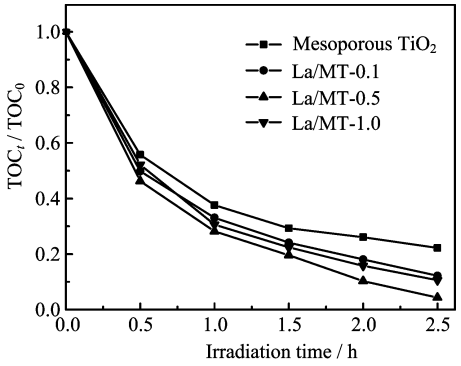

FIG. 7 Degradation of phenol with UV light irradiation for different time.

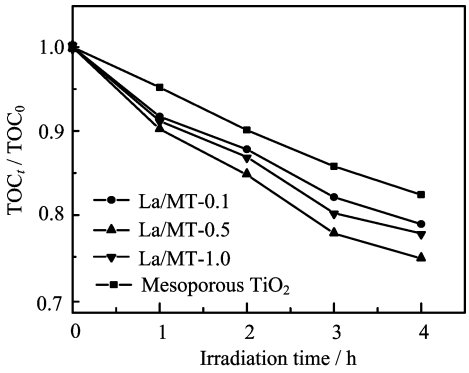

FIG. 8 Degradation of phenol with visible light irradiation for different time.

$$h^+_{vb} + M^{(n-1)+} \rightarrow M^{n+} \quad (7)$$

$$e^-_{cb} + M^{(n+1)+} \rightarrow M^{n+} \quad (8)$$

where M^{n+} is a metal ion dopant. The energy level for $M^{n+}/M^{(n-1)+}$ lies below the conduction band edge (E_{cb}) and the energy level for $M^{(n+1)+}/M^{n+}$ above the valence band edge (E_{vb}).

In this study, photocatalytic reaction mechanism for the degradation of phenol over La/MT photocatalyst was speculated as follows: under light illumination, La-doped TiO_2 photocatalysts are exposed and the electrons are excited from the valence band state to conduction band state. Chen *et al.* reported that the introduction of new impurity states due to the incorporation of La^{3+} decreased the recombination of photogenerated electrons and holes [40]. Hence, in the present study, it was believed that the excited electrons in the conduction band transfered to the La^{3+} states and the holes present in the valence band available for the photocatalytic oxidation of phenol. The rare earth metal (here, La) which usually act as a reservoir for photogenerated electrons, promotes an efficient charge separation in La-doped TiO_2 photocatalysts. In addition, La-doping improved the ultraviolet absorption and the red-shift of the absorption profile (see Fig.4), which was benefit to improve the photocatalytic activity of mesoporous TiO_2, it was also the reason for the high photocatalytic activity of La-doped mesoporous TiO_2.

The increase of the photocatalytic activity with the increase of the content of La-doping might be attributed to the electrons trapped in La sites. The photoactivity of the catalyst increased with an enhancing in the content of La-doping when the content of La-doping was lower than 0.5%. However, the photoactivity of the catalyst decreased when the content of La-doping reached 1.0%. This result can be attributed to the surrounding lanthanum ions, which act as recombination centers for the photogenerated electrons and holes at high doping. The more available lanthanum ions with the higher La-doping concentration will lead to lower photocatalytic activity.

The plot of TOC removal of phenol under visible light is shown in Fig.8. It could be observed that all La-doped samples exhibited higher photocatalytic activity than pure mesoporous TiO_2 under visible light. The photocatalytic activity of pure mesoporous TiO_2 under visible light may be due to the presence of C elements in the heat-treated powders (see Fig.5). From the UV-Vis absorption spectra of samples (Fig.4), it could be seen that the intensity and region of visible light photoabsorption on La-doped mesoporous TiO_2 was stronger and larger, respectively than those of pure mesoporous TiO_2. The strong absorption is beneficial to the photocatalytic activity because the available photons are proportional to photoabsorption. So, the La-doped mesoporous TiO_2 exhibited higher photocatalytic activity than pure mesoporous TiO_2. Among the samples, the La/MT-0.5 showed the best photocatalytic performance. This result should be due to the positive effect of La^{3+} introduction on the photocatalytic activity because the La-doping not only increased the surface area of mesoporous TiO_2 but also extended its photoabsorption to visible light region. The surface area is one of the key factors to control the photocatalytic activity of a photocatalyst. The larger the surface area is, the higher the photocatalytic activity is.

In addition, the concentration of surrounding lanthanum ions influences the activity significantly, because they will act as recombination centers for photogenerated electrons and holes at high doping, thus decreasing the photocatalytic activity. Furthermore, the photoabsorption characters greatly affect the photocatalytic activity of a photocatalyst, since the numbers of absorbed photons directly depend on the absorption property of the photocatalyst. La/MT-0.5 exhibited the highest photocatalytic activity under visible light irradiation, which could be explained by the competition and balance of the three factors above.

IV. CONCLUSION

La-doped mesoporous TiO_2 materials have been synthesized by template method using tetrabutyltitanate

DOI:10.1088/1674-0068/25/01/96-102

($Ti(OC_4H_9)_4$) as precursor and Pluronic P123 as template. La-doping can significantly improve the photoabsorption and slightly increase the surface area of mesoporous TiO_2. The prepared photocatalyst was applied to degrade model contaminated water of phenol. The results showed that the La-doping improved the photocatalytic activity of mesoporous TiO_2 under UV and visible light irradiation, and 0.5% La-doped mesoporous TiO_2 exhibited optimal photocatalytic activity for phenol degradation. The factors such as surface area and photoabsorption affect the photocatalytic activity of La-doped mesoporous TiO_2. It is concluded that incorporation of rare earth metal into the semiconductors has been proven to be a promising approach to improve the photocatalytic activity of semiconductors.

V. ACKNOWLEDGMENT

This work was supported by the National Natural Science Foundation of China (No.41173119).

[1] N. Savage, B. Chwieroth, A. Ginwalla, B. R. Patton, S. A. Akbar, and P. K. Dutta, Sens Actuator B **79**, 17 (2001).
[2] S. Yasuhiro, H. Takeo, and M. Egashira, J. Eur. Ceram Soc. **24**, 1389 (2004).
[3] J. C. Yu, J. Yu, W. Ho, and J. Zhao, J. Photochem. Photobiol. A **148**, 331 (2002).
[4] G. Phani, G. Tulloch, D. Vittorio, and I. Skryabin, Renewable Energy **22**, 303 (2001).
[5] L. Kavan, J. Rathouský, M. Grätzel, V. Shklover, and A. Zukal, Microporous Mesoporous Mater. **44-45**, 653 (2001).
[6] A. Fujishima, T. N. Rao, and D. A. Tryk, J. Photochem. Photobiol. C **1**, 1 (2000).
[7] C. H. Ao, S. C. Lee, Y. Z. Yu, and J. H. Xu, Appl. Catal. B **54**, 41 (2004).
[8] A. Strini, S. Cassese, and L. Schiavi, Appl. Catal. B **61**, 90 (2005).
[9] T. L. Thompson and J. T. Yates, Chem. Rev. **106**, 4428 (2006).
[10] A. C. Rodrigues, M. Boroski, N. S. Shimada, J. C. Garcia, J. Nozaki, and N. Hioka, J. Photochem. Photobiol. A **194**, 1 (2008).
[11] Z. L. Shi, C. Du, and S. H. Yao, J. Taiwan Inst. Chem. Eng. **42**, 652 (2011).
[12] F. Peng, Y. Liu, H. J. Wang, H. Yu, and J. Yang, Chin. J. Chem. Phys. **23**, 437 (2010).
[13] N. Koshitani, S. Sakulkhaemaruethai, Y. Suzuki, and S. Yoshikawa, Ceramics Int. **32**, 819 (2006).
[14] X. X. Fan, T. Yu, L. Z. Zhang, X. Y. Chen, and Z. G. Zou, Chin. J. Chem. Phys. **20**, 733 (2007).
[15] Z. Zou, J. Ye, K. Sayama, and H. Arakawa, Nature **414**, 625 (2002).
[16] R. Asahi, T. Morikawa, T. Ohwaki, K. Aoki, and Y. Taga, Science **293**, 269 (2001).
[17] P. Yang, C. Lu, N. P. Hua, and Y. K. Du, Mater. Lett. **57**, 794 (2002).
[18] W. Choi, A. Termin, and M. R. Hoffmann, J. Phys. Chem. **98**, 13669 (1994).
[19] K. V. Baiju, C. P. Sibu, K. Rajesh, P. Krishna Pillai, P. Mukundan, K. G. K. Warrier, and W. Wunderlich, Mater. Chem. Phys. **90**, 123 (2005).
[20] X. J. Li, D. J. Si, J. Fang, Z. Q Jiang, and W. X. Huang, Chin. J. Chem. Phys. **19**, 539 (2006).
[21] W. Y. Xu, C. Yang, M. B. Luo, L. N. Meng, and G. L. Huang, Adv. Mater. Res. **177**, 96 (2010).
[22] I. Atribak, I. S. Bansanez, A. B. Lopez, and A. G. Garcia, Catal. Communn. **8**, 478 (2007).
[23] T. Ando, T. Wakamatsu, K. Masuda, N. Yoshida, K. Suzuki, S. Masutani, I. Katayama, H. Uchida, H. Hirose, and A. Kamimot, Appl. Surf. Sci. **255**, 9688 (2009).
[24] H. H. Wu, L. X. Deng, S. R. Wang, B. L. Zhu, W. P. Huang, S. H. Wu, and S. M. Zhang, J. Disper. Sci. Technol. **31**, 1311 (2010).
[25] K. Dai, T. Peng, H. Chen, J. Liu, and L. Zan, Environ. Sci. Technol. **43**, 1540 (2009).
[26] H. R. Kim, T. G. Lee, and Y. G. Shul, J. Photochem. Photobiol. A **185**, 156 (2007).
[27] F. B. Li, X. Z. Li, and M. F. Hou, Appl. Catal. B **48**, 185 (2004).
[28] S. J. Gregg and K. S. W. Sing, *Adsorption, Surface Area and Porosity*, 2nd Edn., London: Academic Press, (1982).
[29] J. Yu, Y. Su, B. Cheng, and M. Zhou, J. Mol. Catal. A **258**, 104 (2006).
[30] J. C. Yu, J. G. Yu, W. K. Ho, Z. T. Jiang, and L. Z. Zhang, Chem. Mater. **14**, 3808 (2002).
[31] J. Lin and J. C. Yu, J. Photochem. Photobiol. A **116**, 63 (1998).
[32] K. S. W. Sing, D. H. Everett, R. A. W. Haul, L. Moscou, R. A. Pierotti, J. Rouquerol, and V. T. Siemieniewska, Pure Appl. Chem. **57**, 603 (1985).
[33] F. Rojas, I. Kornhauser, C. Felipe, J. M. Esparza, S. Cordero, A. Dominguez, and J. L. Riccardo, Phys. Chem. Chem. Phys. **4**, 2346 (2002).
[34] Y. Gao, A. W. Xu, and J. Y. Zhu, Chin. J. Catal. **22**, 53 (2001)
[35] L. Wu, J. C. Yu, L. Z. Zhang, X. C. Wang, and W. K. Ko, Solid State Chem. **177**, 2584 (2004).
[36] J. C. Yu, J. G. Yu, H. Y. Tang, and L. Z. Zhang, J. Mater. Chem. **12**, 81 (2002).
[37] K. Baba and R. Hatada, Surf. Coat. Technol. **136**, 241 (2001).
[38] F. Santerre, M. A. E. Khakani, M. Chaker, and J. P. Dodelet, Appl. Surf. Sci. **148**, 24 (1999).
[39] C. Lettmann, K. Hildenbrand, H. Kisch, W. Macyk, and W. F. Maier, Appl. Catal. B **32**, 215 (2001).
[40] W. Chen, D. Hua, T. J. Ying, and Z. J. Mei, Trans. Nonferrous Met. Soc. China **16**, 728 (2006).

DOI:10.1088/1674-0068/25/01/96-102